Acta Cryst. (1966). **21**, 782

The Structure of Bytownite ('Body-Centred Anorthite')

BY S. G. FLEET*, S. CHANDRASEKHAR† AND HELEN D. MEGAW

Crystallographic Laboratory, Cavendish Laboratory, Cambridge, England

(*Received* 10 *March* 1966)

Bytownite (a plagioclase feldspar with composition about $An_{80}Ab_{20}$) closely resembles anorthite in its lattice dimensions and its diffracted intensities, except for the systematic absence of those with $h+k$ odd ('*c*' and '*d*' type). The deduction of a body-centred lattice (whence the previous name, 'body-centred anorthite') is here shown to be incorrect. Three-dimensional electron-density maps and difference maps show conspicuously elongated or doubled Ca/Na peaks and 'half-atom splitting' for other atoms. The results are explained in detail if bytownite has a primitive lattice and a structure very close to (but significantly different from) that of anorthite, and if small anti-phase domains are present with origins related by the vector $\frac{1}{2}(\mathbf{a}+\mathbf{b}+\mathbf{c})$. The evidence for this conclusion, and against other possible explanations of the observed facts, is discussed fully.

Bond lengths and angles (tabulated in full) resemble those in anorthite, with some significant differences. Inequalities of bond lengths and angles within the same tetrahedron are real; an analysis of their resemblances and differences in corresponding tetrahedra in different feldspars suggests an empirical approach to the study of the structural stress systems involved, and emphasizes the difference between the groups comprising microcline, reedmergnerite, and low albite on the one hand, and anorthite, bytownite, and high albite on the other.

Ordering of Si/Al is nearly complete, on the same set of sites as in anorthite. At a closer approximation, a few Al-rich sites show significant differences in their Si content, with extreme values of 0% and 30% against the average value of 13 ± 5% for the rest.

1. Introduction

1.1. *Preamble*

This paper describes an X-ray structural investigation of a plagioclase feldspar with the composition 80% An, 20% Ab. Owing to various circumstances, the work on the structure has been spread over the last twelve years.

The mineral studied was a low feldspar from St. Louis Co., Minnesota (British Museum specimen BM 1921, 33). Feldspars of this composition have frequently been referred to as 'body-centred anorthite' in the past, but in view of the suggestions on nomenclature by Mackenzie (1960), it has been thought best to use the name bytownite.

Following Kempster, Megaw & Radoslovich (1962), we write the feldspar formula AT_4O_8, where A represents the large cation (Na or Ca) and T a 'tetrahedral' cation. The nomenclature used for individual atoms will be that proposed by Megaw (1956).

1.2. *Composition, cell dimensions and space group*

Optical measurements of refractive indices and extinction angles, made by P. M. Game of the British Museum, showed that the specimen was a low plagioclase feldspar of approximate composition 80 ± 2% An, 20 ± 2% Ab (errors estimated). The symmetry is triclinic. With the choice of axial directions which is conventional for feldspars, the unit cell is closely similar to that of primitive anorthite. The cell dimensions, determined by the method of Weisz, Cochran & Cole (1948), using extrapolation against $\sin^2\theta$, were as follows:

$$a=8{\cdot}178\pm0{\cdot}003, b=12{\cdot}870\pm0{\cdot}004, c=14{\cdot}187\pm0{\cdot}005\text{ Å}$$
$$\alpha=93°30'\pm5', \beta=115°54'\pm5', \gamma=90°39'\pm5'$$

(For comparison with the graphs of feldspar cell constants published by Doman, Cinnamon & Bailey (1965) we quote also $\gamma^*=87°35'\pm5'$.) These results are in agreement, to within about twice their standard deviation, with the earlier values, obtained by interpolation from the values published by Cole, Sörum & Taylor (1951), which had been used during the refinement of atomic parameters. The cell contents are

$$8(Ca_{0{\cdot}8}Na_{0{\cdot}2}Al_{1{\cdot}8}Si_{2{\cdot}2}O_8).$$

An investigation of the diffraction pattern of bytownite reveals sharp reflexions of two types only, '*a*' ($h+k$ even, l even) and '*b*' ($h+k$ odd, l odd), in contrast to primitive anorthite where reflexions of types '*c*' ($h+k$ even, l odd) and '*d*' ($h+k$ odd, l even) also occur.

A few weak diffuse streaks were observed on the X-ray photographs. These did not occur systematically, and were always much weaker than '*a*' and '*b*' reflexions. Since they might be the result of zoning or other crystal imperfection and could not be systematized, they were ignored during the structure determination (see, however, § 6.3).

* Now at Department of Mineralogy and Petrology, Cambridge University, England.

† Now at Physics Department, Mysore University, Mysore, India.

The absence of reflexions with $h+k+l$ odd would indicate, for a perfect structure, that its lattice is body-centred. For this reason, and because of the close similarity in other respects to anorthite, the end member of the series, the material studied by us has often in the past been called 'body-centred anorthite'. The provisional assumption of body-centring makes the best starting point for the structure analysis, as it gives a correct empirical description of the effective translational symmetry. Later refinement of the structure, however, produced evidence (*cf.* § 5.5) that the apparent body-centring was an effect of disorder, and therefore the term 'body-centred' in the name of the material is misleading, and must be kept in inverted commas as a warning until it can be dropped completely.

There was no evidence suggesting the absence of a centre of symmetry. The assumption of centrosymmetry was made to begin with, and tested later (*cf.* § 3.3), and was found to be compatible with all the available evidence. The space group of the trial structure is therefore $I\bar{1}$.

2. Method of solution

The problems involved in solving the structure were of a similar kind to those encountered with anorthite (Kempster, Megaw & Radoslovich, 1962). If body-centring is assumed, the four subcells in the unit cell are related in pairs by the body-centring translation $(\mathbf{a}+\mathbf{b}+\mathbf{c})/2$, and thus the problem is reduced to determining the atomic contents and coordinates of the two unlike subcells related by translations $(\mathbf{a}+\mathbf{b})/2$ or $\mathbf{c}/2$. In anorthite, however, all the large cations to be placed were Ca; here one fifth of them are Na, and the possibility of Ca/Na ordering must be admitted. It was assumed, however, that if disorder was initially taken as complete, *i.e.* if all atoms were taken as identical 'average Ca/Na atoms' of composition $Ca_{0\cdot8}Na_{0\cdot2}$, any significant ordering effects would show up during refinement As a consequence, the only differences between subcells are differences of atomic coordinates.

The '*a*' reflexions give the sum of the effects of the two subcells, the '*b*' reflexions their difference. For bytownite, the '*a*' reflexions were very similar in intensity to those of albite, and the albite parameters might reasonably have been taken for the first trial model; they were, however, not known accurately at the time, and it was considered better to use the average parameters from an early refinement of a plagioclase, $An_{72}Ab_{28}$, by Sörum (1951). (Later experience suggests that the parameters of any feldspar will serve satisfactorily as a starting point for the refinement of the average structure of any other.) The outstanding problem was to find the difference parameters to give a good fit for '*b*' reflexions. Fortunately it turned out, as in anorthite, that the atom with the largest difference parameter is the average Ca/Na atom, and therefore a modified heavy-atom technique could be used. Electron-density maps calculated with '*a*' reflexions allowed the Ca/Na difference parameters to be estimated and these difference parameters could be used to calculate signs for '*b*' reflexions. Difference parameters of all the other atoms could then be deduced from the subsequent electron-density and difference maps. The method was found to work: the structure was refined in the usual way. The *R* index for the '*b*' reflexions provided the best guide of successful refinement. Agreement for '*a*' reflexions was good from the start, because of the resemblance of the average subcell to the albite cell.

3. Experimental details

3.1. *Collection of intensities*

Three-dimensional X-ray data were collected by the multiple-film technique on Weissenberg photographs taken with filtered Mo *K* radiation. Data were obtained for zones *hk*0, *h*0*l*, 0*kl*–8*kl*. Intensities were measured visually by comparison with a standard scale of spots made from a well-shaped strong reflexion from the crystal. All reflexions within a cylinder about the *x* axis with length 1·54 r.l.u. and radius 1·01 r.l.u. were recorded. Of these 1959 had finite intensities, and 1600 others not excluded by the body-centring condition were too weak to measure. Table 1 lists the number of type '*a*' and type '*b*' reflexions observed.

3.2. *Corrections to intensities*

Intensities were corrected for Lorentz and polarization effects. No correction was made for absorption because no labour-saving method was available at the time the work was done. The crystal was of irregular shape, $0\cdot3\times0\cdot3\times0\cdot25$ mm. A subsequent rough calculation using a program written by Wells (1961) indicated that the absorption would produce variations of less than 10% on intensities. This was smaller than errors of measurement, and it was not unreasonable to neglect it. A correction was made for errors in measure-

Table 1. *Summary of intensity data*

	Two-dimensional					Three-dimensional		
	*hk*0	*h*0*l*		0*kl*				
		'*a*'	'*b*'	'*a*'	'*b*'	'*a*'	'*b*'	'*a*'+'*b*'
Number of observed reflexions	115	59	16	102	45	1433	526	1959
Number of unobservably weak reflexions within the same reciprocal radius	17	9	42	28	82	380	1257	1637
Total	132	68	58	130	127	1813	1783	3596

ment due to spot shape on higher-layer photographs. Two sets of photographs were taken for each higher layer, so that values for extended and contracted intensities of each spot could be measured. Intensities were then corrected with charts empirically modified from those given by Phillips (1956).

Layers of data were scaled together by comparing the intensities of zones of reflexions common to the *hk*0 and *h*0*l* zero-layer photographs, and to the higher-layer *x*-axis photographs.

No attempt was made to correct for the effect of increasing resolution of the α_1, α_2 doublet with sin θ.

Several strong low-angle reflexions were noticed to be suffering from extinction: the structure amplitudes of these were given calculated values in the electron-density and difference syntheses.

After the average isotropic temperature factor had been determined, F_o values were scaled to F_c by a scaling factor independent of θ. At the final stage of refinement of bytownite, the quantity $\Sigma F_c/\Sigma F_o$ was evaluated for successive shells of reciprocal space and plotted against $\sin^2\theta/\lambda^2$, the square of the mean radius of the shell. The graph was a straight line of zero slope, confirming the correctness of an invariant scale factor.

Final F_o's and F_c's are recorded (Fleet, 1961) and are available on request.

3.3. *Tests for centre of symmetry*

An $N(z)$ test (Howells, Phillips & Rogers, 1950) was performed with the 3596 observable *hkl* reflexions. Fig. 1(*a*) shows the result. The empirical curve has no obvious similarity to either theoretical curve. This is probably because of the large number of '*b*' reflexions with intensities below the observable limit. When the test was carried out with *hk*0 reflexions (all of type '*a*'), a definite centric curve was obtained [Fig. 1(*b*)]. This merely indicates that the average of the two similar halves of the bytownite cell is centrosymmetric. Application of a $P(y)$ test (Ramachandran & Srinivasan, 1959), which may legitimately be applied to all reflexions, gave the value 0·72 for their test ratio N_2/N_1: this is to be compared with theoretical values of 0·78 for a centrosymmetric structure, and 1·96 for a non-centrosymmetric structure. 'Body-centred' bytownite is therefore centrosymmetric.

4. Methods of calculation

4.1. *Atomic scattering factors*

Scattering-factor curves for T, A, and O atoms were constructed by interpolation from those in the literature quoted by Forsyth & Wells (1959). Atoms were assumed to be half-ionized. T cations were taken as average atoms of composition $Si_{0\cdot55}Al_{0\cdot45}$, and A cations as $Ca_{0\cdot8}Na_{0\cdot2}$. An expression of the form $f(x) = A\exp(-ax^2)+B\exp(-bx^2)+C$ was fitted to the curves by the least-squares program written by Forsyth & Wells for use on EDSAC II. Table 2 lists the coefficients.

Table 2. *Scattering-factor constants for half-ionized atoms (Forsyth & Wells (1959) approximation)*

Atom	*A*	*a*	*B*	*b*	*C*
$0\cdot8\ Ca^{+}/0\cdot2\ Na^{0\cdot5+}$	6·470	2·019	7·002	12·81	3·844
$0\cdot55\ Si^{2+}/0\cdot45\ Al^{1\cdot5+}$	7·645	2·717	2·201	52·43	1·929
O^{-}	4·322	6·983	3·243	36·48	1·434

4.2. *Refinement methods*

Standard difference-map and electron-density-map methods of refinement were used at the start of the work. Later, several cycles of refinement were carried out with full three-dimensional data, using a differential Fourier program written for EDSAC II by Wells (1961).

Separate isotropic temperature factors were applied to different classes of atom (not to each atom individually), and were refined in the usual way.

5. Structure analysis

5.1. *Refinement of the average structure*

At the start of the work, '*b*' reflexions were neglected altogether, and the coordinates of nearly identically situated atoms in the two albite-like halves of the unit cell were effectively averaged. Signs calculated from the refinement of Sörum (1951), referred to above (§ 2), were applied to '*a*' reflexions, and the 'average' structure was refined from this starting point by standard Fourier techniques using two-dimensional data only. There was much overlap, but a few peaks were well resolved in each projection. At the limit of refinement

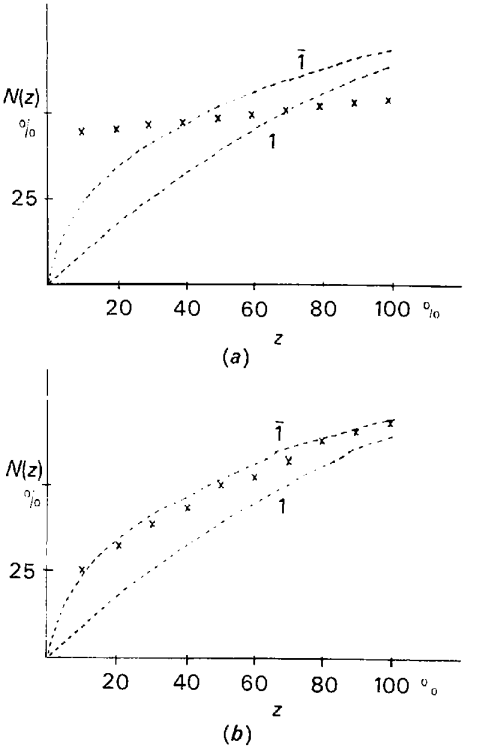

Fig. 1. $N(z)$ plot (*a*) for all *hkl* reflexions (including types '*a*' and '*b*'), (*b*) for *hk*0 reflexions (all of type '*a*').

it was clear that many peaks were elliptical in shape. These ellipticities were an indication of the distances through which atoms had to be shifted from average positions to give the 'body-centred' structure. It was noticed that the Ca/Na peak was more markedly elliptical than any other. Fig. 2 shows a projection of the average structure on (100) at this stage: the ellipticity of Ca/Na can be clearly seen.

5.2. *Determination of the 'body-centred' structure*

Since the A atoms are heavier than either T or O atoms, the possibility of using the heavy-atom method of sign determination suggested itself.

The separation of Ca/Na from its average position was judged from electron-density maps of the average structure, assuming that the elliptical peak was the sum of two circular peaks. This was first done in the (100) projection, in which Ca/Na ellipticity was most pronounced. Structure factors for $0kl$ 'a' reflexions were then calculated with individual coordinates for Ca/Na atoms, and average coordinates for T and O atoms. The R index for 'a' reflexions went down abruptly by about 3·5%. Using R as a criterion, the best value for the Ca/Na splitting was determined after three or four trials. The Ca/Na splitting was next estimated in a similar manner in the (001) projection. In this case the estimation was harder because the ellipticity of the average peak was less marked.

Next, the correct choice of symmetry centre had to be made; this was equivalent to the allocation of correct signs to the difference parameters of individual

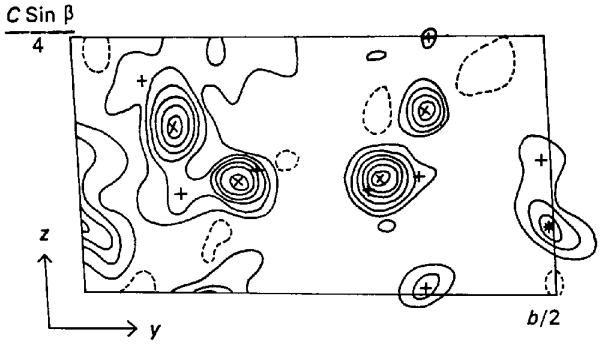

Fig. 2. Electron-density map of average structure, [100] projection. Ca/Na position marked *, Si/Al positions ×, O positions +.

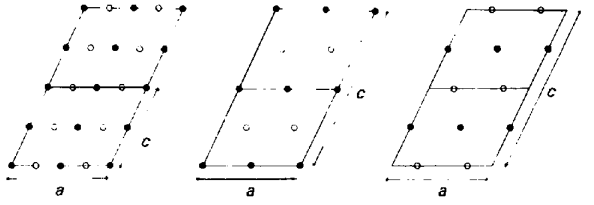

• *Symmetry centres at* $y = 0, 1/2$

○ *Symmetry centres at* $y = 1/4, 3/4$

Fig. 3. Possible locations of symmetry centres, relative to origin fixed with respect to structural features, Left: two cells of albite structure. Centre and right: one cell of 14 Å body-centred structure (two different possibilities).

Ca/Na atoms. As long as the average structure – similar to albite – was being refined, it was reasonable to assume (by analogy with other C-face-centred feldspar structures) that there were symmetry centres at 000 and $00\frac{1}{4}$ (together with others derived from each of them by lattice translations) [Fig. 3(*a*)]. On passing to the 'body-centred' structure only one of the two sets could be retained, either 000 as in Fig. 3(*b*) or $00\frac{1}{4}$ as in Fig. 3(*c*). These are physically different choices.

To decide between them, structure factors of $0kl$ 'b' reflexions were calculated for each of the two models. The issue had not been prejudged in calculating structure factors of 'a' reflexions as described above, because they depend only on the magnitudes and not on the signs of the difference parameters, and are therefore the same for both models. Only the Ca/Na contributions to the 'b' reflexions could as yet be calculated, and therefore we could only look for discrimination to those reflexions in which the Ca/Na contributions are relatively large, *i.e.* to strong reflexions. Of 16 such reflexions (restricted, for reasons not now considered valid, to a reciprocal radius less than 0·2), 5 showed little difference between the two models, 7 favoured the centre at 000 strongly and 2 others fairly strongly, and only 2 favoured the centre at $00\frac{1}{4}$. The centre at 000 was therefore taken to be correct. Further work confirmed this choice (*cf.* § 6.1).

Signs of some 'b' reflexions were now available. Electron-density and difference maps of the 'body-centred' structure were calculated for projections along each of the principal crystallographic axes. The x axis being the shortest, the (100) projection was the most informative. There was considerable overlapping of the peaks (an idea of the extent of overlap may be had from Fig. 5 given later), but the centres of a few atoms could be fixed fairly accurately in each projection. Information derived from one projection was used to locate approximately the centres of the overlapping atoms in the other two. At the start of the refinement, most signs of 'a' reflexions were correctly known but those of 'b' reflexions were still uncertain. $F_o - F_c$ syntheses were therefore to be used as difference syntheses (Cochran, 1951) for 'a' reflexions, and as 'error' syntheses (Crowfoot, Bunn, Rogers-Low & Turner-Jones, 1949) for 'b' reflexions. All 'a' reflexions were included in the syntheses, but only those 'b' reflexions with small F_o and relatively large F_c were considered in the early stages. Separate F_o and F_c syntheses were made together with each $F_o - F_c$ synthesis. They proved helpful because the non-circularity of peaks in F_o maps could be clearly seen by comparison with corresponding peaks in the F_c maps.

Several cycles of refinement were carried out on these lines. Reliability indices at this stage were:

	'a' type	'b' type	'a' and 'b' types
$0kl$	24·8%	55%	29·0%
$h0l$	18·2	46	20·0
$hk0$	25·6		

R values for '*a*' reflexions had improved considerably (from initial values of 50% for 0*kl* and 26% for *h*0*l*), but those for '*b*' reflexions were still very high.

5.3. '*Half*-Ca/Na' *atoms*

In the electron-density map on (100) it was noticed that both Ca/Na peaks were still markedly elliptical. At first it was assumed that this was due to overlap, for in this projection $O_A(2000)$ and $O_A(2zi0)$ fall quite near to Ca/Na(000) and Ca/Na(*zi*0). That this was not so became clear from F_o-F_c syntheses. Fig. 4 shows the actual contours in the electron-density and difference maps. The shape of the contours suggests one of the two possibilities:

(i) A very anisotropic temperature factor,
(ii) Two (equally probable?) cation sites corresponding to each peak.

The latter alternative was thought to be more likely because the anisotropy of the peak appeared too large to be the result of thermal motion. A similar ellipticity of Ca/Na cation has been observed in several other plagioclase feldspars, notably in both low and high albite (Ferguson, Traill & Taylor, 1958; Williams & Megaw, 1964) in which the Na peak is very elliptical. Before further refinement could be carried on, it was necessary to estimate the approximate separation of the two Ca/Na sites corresponding to each peak. This was done by inspection of difference maps. The separation was greater for Ca/Na(000) than for Ca/Na(*zi*0). Each Ca/Na peak was then approximated by two 'half' Ca/Na atoms representing the two (equally probable?) sites corresponding to the peaks. The *R* index for '*a*' reflexions dropped by 3% showing that refinement was proceeding satisfactorily. Further refinement was then carried through using the 'half' Ca/Na atoms. Final *R* values at the limit of two-dimensional refinement are given below. When comparing these with the *R* indices quoted above, it is important to note that computational methods were changed during the two-dimensional refinement, when EDSAC II became available.

	'*a*' type	'*b*' type	'*a*' and '*b*' types
0*kl*	9·8%	20·2%	10·8%
*h*0*l*	8·2	14·3	9·8
*hk*0	8·7	–	8·7

The final two-dimensional electron-density maps are given in Fig. 5. In the (100) and (010) projections, the map consists of two halves which are almost but not quite identical. Starting from the average (albite-type) structure in which the two halves are exactly identical, small but significant differences in coordinates have been achieved. These small differences were responsible for the weak '*b*' reflexions. The (001) projection does not resemble the other two in this respect because the doubling of the unit cell takes place along the *c* axis.

Final coordinates and isotropic temperature factors at the limit of two-dimensional refinement are given in Table 3.

5.4. *Refinement of bytownite in three dimensions*

Further refinement of the structure was carried out with full three-dimensional data on EDSAC II with a differential-Fourier program written by Wells (1961). Isotropic temperature factors applied to each group of atoms were refined by the program, as was the single factor by which F_o's were scaled to F_c's. Reflexions for which $|F_o|-|F_c|$ were greater than 10 on an absolute scale or for which F_o/F_c lay outside the range $\frac{1}{2}$ to 2 were rejected and printed out by the program. The number of rejected reflexions fell from 252 to 42 in the course of the refinement. 15 low-angle reflexions suffering from extinction were given F_c values throughout.

Several cycles of refinement reduced the three-dimensional *R* index to 11·8%, at which stage refinement had ceased. The standard deviation of electron-density calculated from Cochran's formula [Lipson & Cochran, 1953, equation (308·3)] was 0·23 e.Å^{-3}. Coordinates and temperature factors at this point are given in Table 3. The coordinates represent the best 'body-centred' fit to the bytownite intensities.

So far, the only striking evidence that this is not the true structure has been the ellipticity of the two Ca/Na peaks and the need to approximate each of them with two 'half'-atoms. It is perhaps worth noting that the temperature factor of 1·06 Å^2 for oxygen peaks is rather larger than in other simple feldspars, possibly suggesting that these peaks are averages over more than one site.

5.5. *Three-dimensional electron-density and difference maps*

Electron-density and difference-map sections were calculated at intervals of 1/64th cell edges with the coordinates in Table 3(*a*), column 3.

Sections of the electron-density map passing as nearly as possible through the centres of the two Ca/Na

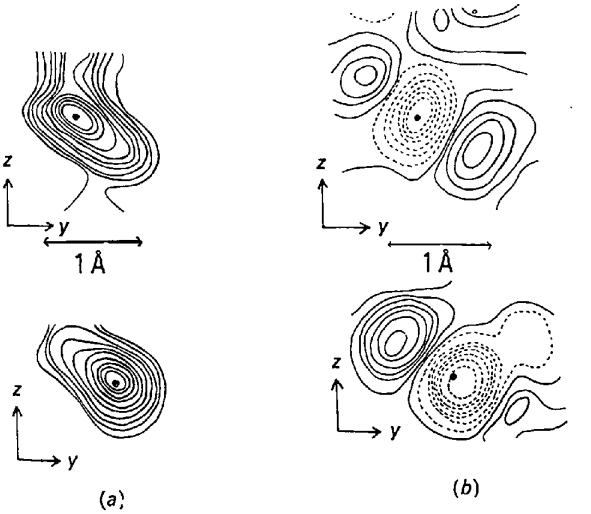

Fig. 4. [100] projection of the two Ca/Na atoms: (*a*) electron-density map, (*b*) difference map. Ca/Na(000) upper, Ca/Na (*z*00) lower in both (*a*) and (*b*).

peaks are shown in Fig. 6. Ca/Na(000) can be seen to be split into two well-resolved 'half'-sites (about 0·85 Å apart), corresponding to two possible positions for the Ca/Na atom. Ca/Na ($z00$) is pear-shaped, but has been approximated by two 'half'-atoms 0·43 Å apart. Sections through the other atoms were plotted out, but none of them had noticeably elliptical peaks.

Fig. 7 shows sections through atoms on the three-dimensional difference map (the arrows through atomic centres will be referred to in § 6.3). Many sections show clear evidence of anisotropies. Sections through oxygen atoms showed similar, though less marked, evidence of anisotropies*. It must be repeated that isotropic temperature factors had only been applied to groups of atoms, not to individual ones: atoms often lie in non-zero regions in the map as a result.

It was possible to estimate the major direction of anisotropy of each atom from the difference map. Many anisotropies were large, corresponding to mean square displacements greater than 0·2 Å. In view of this, it is suitable at this point to discuss possible reasons for them.

* Diagrams showing sections through the oxygen atoms can be made available on request.

6. Discussion of anisotropies of atoms in bytownite

6.1. *Possibility of wrongly imposed symmetry elements*

Anisotropies would arise if the centre of symmetry were truly at $(00\frac{1}{4})$ and its related sites instead of at the cell origin. To test this, the origin was shifted by $c/4$,

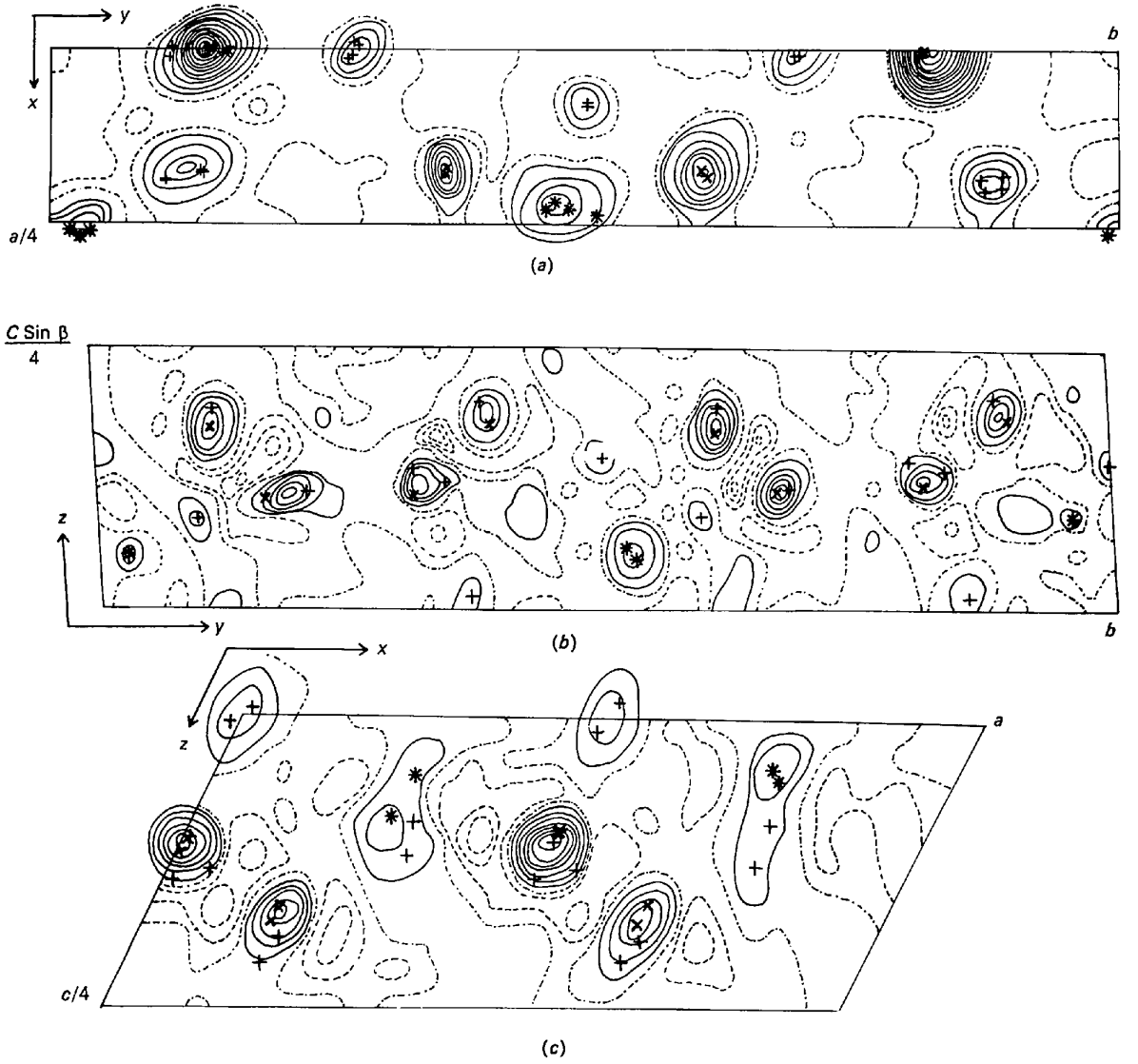

Fig. 5. Electron-density projections at end of two-dimensional refinement: (*a*) [001], (*b*) [100], (c) [010]. Half-atom Ca/Na marked *, Si/Al marked ×, O marked +. Electron-density contours are at regular arbitrary intervals; the positive contours are solid, negative contours dashed and zero contours chained.

Table 3. *Position parameters and thermal parameters*

(*a*) Position parameters as fractions of cell edge $\times 10^4$: for each atom the figures in three successive rows are *x*, *y*, *z* respectively

1 Atom	2 2-D refinement		3 3-D refinement, *b* . *c*. approximation (except for Ca/Na)		4 Final half-atom refinement		5 Refinement from anorthite trial structure	
					α	β		
Ca/Na(000)	2673	2678	2664	2745	2665	2746	2666	7747
	9851	0261	9837	0313	9838	0316	9839	5320
	0872	0535	0860	0485	0860	0478	0858	5476
Ca/Na(*z*00)	2677	2718	2710	2624	2707	2633	2706	7635
	0406	0213	0392	0164	0380	0178	0377	5181
	5378	5532	5402	5591	5414	5580	5415	0577
T_1(0000)	0055		0074		0089	0083	0091	5055
	1620		1591		1600	1584	1600	6584
	1063		1047		1045	1035	1045	6035
T_1(0*z*00)	0049		0033		0075	9993	0075	4995
	1630		1657		1621	1691	1621	6687
	6091		6100		6110	6106	6110	1109
T_1(*m*000)	0038		9992		9931	0077	9933	5078
	8144		8151		8146	8157	8147	3155
	1181		1188		1181	1206	1183	6206
T_1(*mz*00)	0045		0060		0063	0038	0058	5033
	8133		8183		8152	8209	8154	3207
	6166		6129		6140	6106	6138	1103
T_2(0000)	6822		6886		6857	6928	6857	1926
	1105		1112		1119	1110	1124	6114
	1600		1579		1517	1651	1514	6661
T_2(0*z*00)	6819		6786		6826	6734	6825	1726
	1068		1060		1043	1070	1039	6068
	6588		6588		6640	6530	6642	1521
T_2(*m*000)	6784		6774		6773	6757	6766	1761
	8796		8814		8824	8808	8826	3805
	1812		1819		1868	1757	1871	6752
T_2(*mz*00)	6798		6842		6805	6876	6805	1873
	8776		8756		8722	8785	8722	3788
	6776		6761		6726	6811	6723	1812
O_A(1000)	0069		0117		0238	9936	0251	4924
	1249		1275		1276	1273	1270	6275
	9948		9920		9951	9869	9950	4865
O_A(1*z*00)	0045		9957		9841	0123	9844	5129
	1250		1280		1263	1293	1263	6289
	4890		4880		4834	4938	4828	9945
O_A(2000)	5744		5782		5784	5765	5776	0760
	9954		9911		9923	9900	9924	4896
	1351		1396		1438	1348	1437	6345
O_A(2*z*00)	5758		5742		5748	5756	5749	0762
	9889		9911		9908	9914	9907	4915
	6383		6364		6390	6367	6392	1367
O_B(0000)	8037		8237		8113	8328	8114	3343
	1010		1000		1040	0962	1034	5956
	0987		0929		0839	0997	0839	6004
O_B(0*z*00)	8004		7994		8082	7918	8084	2917
	1030		1034		1019	1045	1016	6045
	5910		5943		6018	5868	6015	0861
O_B(*m*000)	8253		8128		8174	7991	8167	2989
	8462		8509		8498	8562	8502	3560
	1214		1318		1403	1144	1411	6141
O_B(*mz*00)	8201		8162		8091	8361	8087	3366
	8452		8560		8512	8587	8509	3587
	6136		6105		6039	6276	6045	1286
O_C(0000)	0151		0121		0106	0069	0109	5071
	2804		2802		2812	2819	2811	7813
	1417		1358		1360	1320	1355	6318
O_C(0*z*00)	0151		0134		0179	0126	0187	5129
	2866		2967		2936	2985	2931	7982
	6446		6434		6462	6458	6463	1465
O_C(*m*000)	0058		0081		0035	0144	0026	5145
	6856		6800		6807	6801	6804	1796
	1038		1098		1082	1109	1080	6105

Table 3 (*cont.*)

1 Atom	2 2-D refinement	3 3-D refinement, b-c approximation (except for Ca/Na)	4 Final half-atom refinement		5 Refinement from anorthite trial structure	
			α	β		
$O_C(mz00)$	0074	0127	0112	0115	0100	5145
	6914	6915	6886	6950	6888	1976
	6027	6008	6040	5982	6032	6105
$O_D(0000)$	1959	1912	1810	1963	1803	6955
	1065	1066	1079	1060	1077	6053
	1855	1878	1924	1831	1916	6822
$O_D(0z00)$	1984	2023	2108	1976	2113	6967
	1030	1046	1065	1034	1067	6034
	6902	6898	6877	6942	6877	1950
$O_D(m000)$	1814	1959	2026	1906	2024	6903
	8711	8677	8718	8642	8717	3644
	2183	2200	2102	2261	2107	7274
$O_D(mz00)$	1863	1857	1754	1955	1752	6960
	8660	8633	8577	8698	8578	3699
	7150	7100	7193	7044	7182	2036

(*b*) Final structure

Coordinates of atoms in first half-cell as in column 4(α) of Table 3(*a*); in second half-cell, derived by adding 5000 to each of the values listed in column 4β, and changing the symbol by that for the body-centring translations.

Ca/Na(000)	2665	Ca/Na(0*i*0)	7746	$O_A(2z00)$	5748	$O_A(2zi0)$	0756
	9838		5316		9908		4900
	0860		5478		6390		6348
Ca/Na(*z*00)	2707	Ca/Na(*zi*0)	7633	$O_B(1000)$	8113	$O_B(10i0)$	3328
	0380		5178		1040		5962
	5414		0580		0839		5997
$T_1(0000)$	0089	$T_1(00i0)$	5083	$O_B(0z00)$	8082	$O_B(0zi0)$	2918
	1600		6584		1019		6045
	1045		6035		6018		0868
$T_1(0z00)$	0075	$T_1(0zi0)$	4993	$O_B(m000)$	8174	$O_B(m0i0)$	2991
	1621		6691		8498		3562
	6110		1106		1403		6144
$T_1(m000)$	9931	$T_1(m0i0)$	5077	$O_B(mz00)$	8091	$O_B(mzi0)$	3361
	8146		3157		8512		3587
	1181		6206		6039		1276
$T_1(mz00)$	0063	$T_1(mzi0)$	5038	$O_C(0000)$	0106	$O_C(00i0)$	5069
	8152		3209		2812		7819
	6140		1106		1360		6320
$T_2(0000)$	6857	$T_2(00i0)$	1928	$O_C(0z00)$	0179	$O_C(0zi0)$	5126
	1119		6110		2936		7985
	1517		6651		6462		1458
$T_2(0z00)$	6826	$T_2(0zi0)$	1734	$O_C(m000)$	0035	$O_C(m0i0)$	5144
	1043		6070		6807		1801
	6640		1530		1082		6109
$T_2(m000)$	6773	$T_2(m0i0)$	1757	$O_C(mz00)$	0112	$O_C(mzi0)$	5115
	8824		3808		6886		1950
	1868		6757		6040		0982
$T_2(mz00)$	6805	$T_2(mzi0)$	1876	$O_D(0000)$	1810	$O_D(00i0)$	6963
	8722		3785		1079		6060
	6726		1811		1924		6831
$O_A(1000)$	0238	$O_A(10i0)$	4936	$O_D(0z00)$	2108	$O_D(0zi0)$	6976
	1276		6273		1065		6034
	9951		4869		6877		1942
$O_A(1z00)$	9841	$O_A(1zi0)$	5123	$O_D(m000)$	2026	$O_D(m0i0)$	6906
	1263		6293		8718		3642
	4834		9938		2102		7262
$O_A(2000)$	5784	$O_A(20i0)$	0765	$O_D(mz00)$	1754	$O_D(mzi0)$	6955
	9923		4900		8577		3698
	1438		1348		7193		2044

(*c*) Temperature factors in Å^2 (assumed isotropic, and the same for chemically similar atoms).

	2-D refinement	3-D refinement
Ca/Na	0·75	0·90
T	0·40	0·37
O	1·15	1·06

and a centre was assumed at the new origin. This meant averaging coordinates that were previously only approximately related by a centre at $(00\frac{1}{4})$ in such a way that the (000) centre was lost. Ca/Na atoms were assumed to be normal (unsplit) atoms because it was desired to test whether their ellipticities would vanish with the new choice of centre. The initial three-dimensional R index was 22·6%. Refinement reduced R to 19·2%, as compared with 11·8% for the (000) centre. Two-dimensional maps indicated that Ca/Na ellipticities remained. Bond lengths for T–O bonds were calculated with the 19·2% coordinates and found to show much wider variations within a tetrahedron than did those with the coordinates in Table 3(*a*), column 3. It was clear that the anisotropies were not the result of a wrong choice of centre.

It was also possible that bytownite might lack a true centre of symmetry. To test for this, coordinates were selected for Ca/Na atoms so that the two observed anisotropic peaks would be produced on imposing a centre at the cell origin. The structure was refined as non-centrosymmetric from this starting point, and gave a best R value of 16·5% on three-dimensional data. Again T–O bond lengths had a much wider scatter than those from the coordinates in Table 3(*a*), column 3. It was concluded that the structure had a centre of symmetry, and that the refinement with centre at cell origin gave the best fit, bond lengths and intensities both considered.

6.2. *Possibility of thermal motion*

The Ca/Na peaks have an ellipticity represented by two 'half'-sites with 0·85 and 0·43 Å separation respectively. These separations are much too large to be the result of thermal motion.

Oxygen and Si/Al peaks have anisotropies corresponding to root mean square displacements of as much as 0·20 Å in some cases. Again many anisotropies are too large to be caused by thermal motion.

Although thermal motion may well contribute to the observed anisotropies, the size of many of them can only be explained if O, T, and A peaks are averages over two or more possible sites. Bytownite must, therefore, have a different structure in different parts of a crystal, not only as regards A positions, but as regards O and T sites as well. The fact that the isotropic temperature factors, 1·06 Å^2 for oxygen, 0·37 Å^2 for T atoms, are rather larger than those for similar well-refined feldspar structures is also explained, because they will incorporate a 'spread' factor if T and O peaks are really averages over two or more possible sites.

6.3. *An explanation of the anisotropies*

Inspection of the three-dimensional difference map showed:

(i) that small shifts ($\leq$0·001 Å) were still indicated for some atoms;

(ii) that individual isotropic temperature factors differed a great deal from the group means;

(iii) that many atoms were strikingly anisotropic, the nature of the anisotropic regions around the atoms suggesting that the oxygen and Si/Al peaks could be fitted by two 'half'-atoms as the Ca/Na peaks had been.

Each atom was therefore represented by two 'half'-atoms with a separation estimated by inspection of the three-dimensional maps, and the structure was refined from this starting point with Wells's differential-Fourier program. Temperature factors were kept fixed during the refinement. The initial R value was 12·5% and the final one 11·1%. The final standard deviation of electron density $\sigma(\varrho_0)$ was 0·20 e.Å^{-3} (*cf.* the value 0·23 e.Å^{-3}, obtained when only Ca/Na were given 'half'-atom representation in § 5.4). Table 3(*a*), column 4 lists the final 'half'-atom coordinates. Fig. 7 has the final magnitude and directions of atomic splittings marked on the three-dimensional difference-map sections. Several splittings failed to tally exactly with the obvious directions of anisotropies on the map: this was probably because the difference map contained spurious peaks, as a result of inaccurate data and incomplete refinement. It is not possible to say whether a better fit could be obtained using more 'fractional' sites than two for each peak. Certainly the fit with two 'half'-sites is a good first approximation.

At this stage, the 104 atoms in the unit cell of bytownite are described in terms of 26 independent half-atom pairs, each repeated by the operation of a centre of symmetry and the body-centring translation. We have

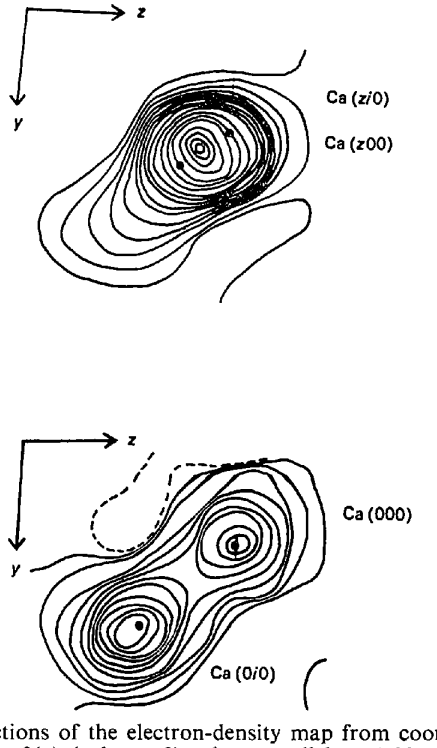

Fig. 6. Sections of the electron-density map from coordinates of Table 3(*a*) (column 3) taken parallel to (100) through Ca/Na peaks. Individual labels of half-atom peaks are as allocated later; contour interval is 3 e.Å^{-3}.

shown in § 6.1 that lack of a centre of symmetry cannot explain the 'half'-atom splitting; the other obvious possibility is to reject the body-centring. Then, taking identical pairs of 'half'-atom sites symmetrical about x, y, z and $\frac{1}{2}+x, \frac{1}{2}+y, \frac{1}{2}+z$ respectively, we must place an atom on one site of the first pair and the complementary site of the second pair; and this choice must be made independently for the 26 independent pairs, giving 2^{26} different configurations. Since, however, it is arbitrary which we regard as the 'first pair' for initial choice, half the configurations only differ from the other half by a displacement $(\mathbf{a}+\mathbf{b}+\mathbf{c})/2$, *i.e.* they are not distinct 'structures' but translation-related locations of the same structure. All configurations, however, give the same F_c values for '*a*' and '*b*' reflexions, and from the diffraction evidence it is impossible to distinguish between them.

The absence of '*c*' and '*d*' reflexions can be explained by assuming the existence of out-of-phase domains. Consider two configurations X and Y with identical

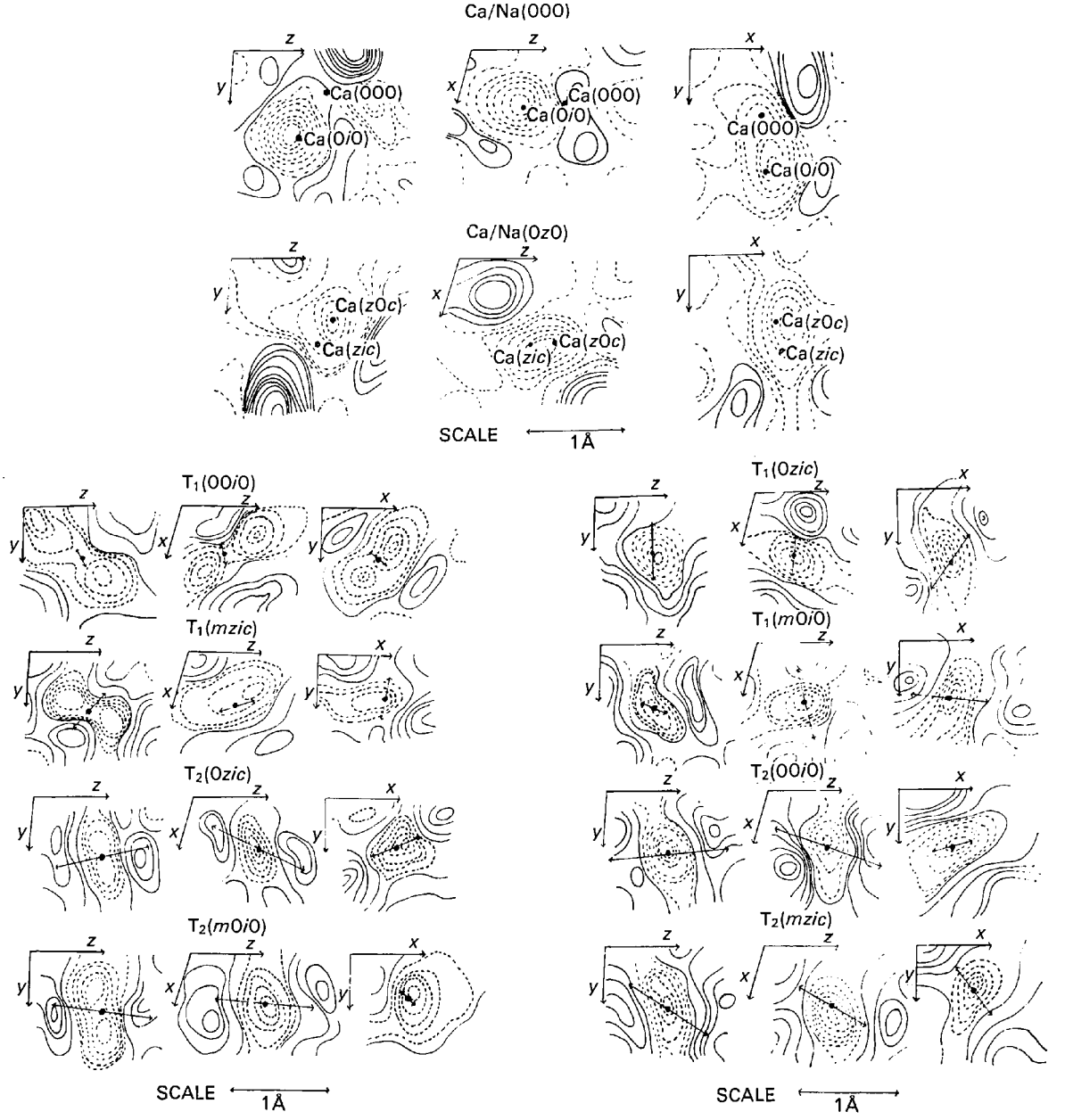

Fig. 7. Sections of difference maps from coordinates of Table 3(*a*) (column 3) taken in directions indicated through cation centres. Upper part of figure: Ca/Na. Lower part: T_1 and T_2. Electron-density contours are at intervals of 0·15 e.Å^{-3}; the positive contours are solid, negative contours dashed and zero contours chained. Arrows show the direction of the 'splitting' of the atoms after subsequent refinement with 'half-atoms'; the length of these lines is proportional to the magnitude of the 'splitting' but on a scale three times that of the maps. (x, z sections are drawn with y pointing downwards.)

structures but origins differing by $(\mathbf{a}+\mathbf{b}+\mathbf{c})/2$. If the crystal consists of a coherently-scattering juxtaposition of small domains of the two, reflexions with $h+k+l$ odd will be out of phase for *X* and *Y*, and will be diffuse and perhaps unobservable, while those for $h+k+l$ even will remain sharp. An out-of-phase domain texture can, therefore, explain the apparent body-centring. Physically, such an explanation is reasonable because of the close resemblance which must exist between two halves of the unit cell along the [111] direction, as shown by the small magnitudes of the 'half'-atom splittings; a mistake in the sequence is not unlikely.

We are not here concerned with the detailed distribution of mistakes, but merely point out that they could in principle explain the observed effects. If the faults were not completely random, one might expect weak streaks in the '*c*' and '*d*' positions; the few weak streaks observed (*cf.* § 1.2) were not systematically in such positions, and, as even the longest-exposed photographs did not give systematic effects, no attempt was made to follow them up in further detail.

Further support for this explanation of the absence of '*c*' and '*d*' reflexions comes from the existence of the so-called 'transitional anorthites' of compositions between $An_{100}Ab_0$ and $An_{80}Ab_{20}$. These are characterized by diffuse '*c*'-type reflexions and diffuse or absent '*d*'-type reflexions. In some cases the degree of diffuseness can be attributed to 'thermal state', and is capable of reduction by suitable annealing; in other cases, in which any available heat treatment only increases the diffuseness, it depends on composition, increasing steadily with albite content. These variations of diffuseness can be explained by postulating the same (or very nearly the same) primitive structure over the whole range, with a changing concentration of anti-phase boundaries. A preliminary discussion of a transitional anorthite An_{100} has been given by Ribbe & Megaw (1962).

It remains to decide between the 2^{25} configurations or 'structures' compatible with the diffraction evidence. One possible criterion, not dependent on comparison with other structures, would be to see which of them had the more regular tetrahedra. Bond lengths from each half-Si/Al (T) site to each half-O site surrounding it are given in Table 4. It can be seen on inspection that there will be a great many possible configurations with fairly regular T–O tetrahedra. It is likely that there will be real deviations of bond length within each

Table 4. *Bond lengths from each 'half-*T' *atom to each 'half-oxygen' surrounding it.*

The labels α and β are the same as those used in Table 3(*a*), column 4, where the coordinates of the 'half-atoms' are recorded.

	$T_1(0000)\alpha$	$T_1(0000)\beta$		$T_2(m000)\alpha$	$T_2(m000)\beta$
$O_A(1000)\alpha$	1·639	1·640	$O_A(2000)\alpha$	1·648	1·642
β	1·644	1·639	β	1·654	1·635
$O_B(0000)\alpha$	1·658	1·625	$O_B(m000)\alpha$	1·600	1·483
β	1·621	1·592	β	1·534	1·617
$O_C(0000)\alpha$	1·594	1·609	$O_C(0zi0)\alpha$	1·601	1·593
β	1·590	1·614	β	1·589	1·582
$O_D(0000)\alpha$	1·600	1·606	$O_D(0z0c)\alpha$	1·602	1·743
β	1·636	1·653	β	1·534	1·672
	$T_1(mz00)\alpha$	$T_1(mz00)\beta$		$T_1(0z00)\alpha$	$T_1(0z00)\beta$
$O_A(1z0c)\alpha$	1·642	1·562	$O_A(1z00)\alpha$	1·766	1·813
β	1·675	1·601	β	1·519	1·753
$O_B(mz00)\alpha$	1·628	1·607	$O_B(0z00)\alpha$	1·745	1·727
β	1·588	1·569	β	1·783	1·765
$O_C(mz00)\alpha$	1·628	1·699	$O_C(0z00)\alpha$	1·725	1·633
β	1·560	1·623	β	1·786	1·697
$O_D(mz00)\alpha$	1·587	1·601	$O_D(0z00)\alpha$	1·728	1·816
β	1·633	1·636	β	1·701	1·791
	$T_2(0z00)\alpha$	$T_2(0z00)\beta$		$T_1(m000)\alpha$	$T_1(m000)\beta$
$O_A(2z00)\alpha$	1·635	1·648	$O_A(100c)\alpha$	1·760	1·751
β	1·615	1·636	β	1·748	1·726
$O_B(0z00)\alpha$	1·619	1·563	$O_B(m000)\alpha$	1·660	1·761
β	1·697	1·616	β	1·657	1·754
$O_C(m0i0)\alpha$	1·689	1·598	$O_C(m000)\alpha$	1·725	1·734
β	1·616	1·524	β	1·747	1·744
$O_D(m00c)\alpha$	1·619	1·758	$O_D(m000)\alpha$	1·755	1·663
β	1·463	1·600	β	1·751	1·665
	$T_2(0000)\alpha$	$T_2(0000)\beta$		$T_2(mz00)\alpha$	$T_2(mz00)\beta$
$O_A(2000)\alpha$	1·736	1·724	$O_A(2z00)\alpha$	1·747	1·710
β	1·754	1·744	β	1·755	1·724
$O_B(0000)\alpha$	1·686	1·808	$O_B(mz00)\alpha$	1·731	1·790
β	1·672	1·766	β	1·654	1·703
$O_C(mzi0)\alpha$	1·654	1·718	$O_C(00i0)\alpha$	1·681	1·768
β	1·710	1·786	β	1·693	1·783
$O_D(mz0c)\alpha$	1·696	1·542	$O_D(000c)\alpha$	1·746	1·640
β	1·843	1·668	β	1·855	1·732

tetrahedron in any case, and it is clear that it will be impossible on bond-length evidence to decide which atomic array is the most likely when the lengths change so little from one possibility to another.

At this stage it is necessary to depart from a completely rigorous approach, and to test a reasonable hypothesis against the data. This is an hypothesis which suggests itself as a consequence of the work of Megaw (1960, § 5.1) on intermediate plagioclase structures. We note that there is a striking resemblance in coordinates between primitive anorthite and one of the particular solutions of bytownite. (Cell dimensions change so little between anorthite and bytownite that coordinates may be directly compared.) The 'half-atom' coordinates for Ca/Na atoms in bytownite are:

	x	*y*	*z*
Ca/Na(000)	0.2746	0.0316	0.0478
	0.2665	0.9838	0.0860
Ca/Na(*z*00)	0.2633	0.0178	0.5580
	0.2707	0.0380	0.5414

(fractions of a cell edge);

and of course there are four other 'half'-atoms related to these by body-centring. If we select four particular sites for Ca/Na atoms in the bytownite cell, choosing one from each pair of 'half'-sites thus:

	x	*y*	*z*
Ca/Na(000)	0.2665	0.9838	0.0860
Ca/Na(0*i*0)	0.7746	0.5316	0.5478
Ca/Na(*z*00)	0.2707	0.0380	0.5414
Ca/Na(*zi*0)	0.7633	0.5178	0.0580

we obtain positions extremely similar to the Ca sites in anorthite:

Ca(000)	0.2647	0.9844	0.0873
Ca(0*i*0)	0.7732	0.5354	0.5422
Ca(*z*00)	0.2684	0.0312	0.5438
Ca(*zi*0)	0.7636	0.5067	0.0740

There is a similar striking resemblance between the anorthite T and O coordinates and those of one of each pair of T and O 'half'-sites in bytownite. Reference to Table 3, column 4, and to the Table 8 of Kempster, Megaw & Radoslovich (1962), will confirm this. It is therefore possible to select a structure for bytownite which is very closely similar to that of primitive anorthite. This is one particular solution from the 2^{25} possibilities. The coordinates of this particular solution are given in Table 3(*b*).

It is of course possible, as far as the diffraction evidence goes, that one of the other 2^{25} structures is the correct one. The particular solution resembling primitive anorthite has been chosen because it is consistent with a continuous structural change from anorthite to bytownite, as silicon and sodium are substituted for aluminium and calcium.

The evidence for the relationship to primitive anorthite can be displayed by the use of a different refinement procedure. In this, primitive anorthite was taken as the trial structure, and refinement was carried out from the F_{obs} of bytownite putting $F_{calc}=0$ for reflexions with $h+k+l$ odd. The coordinates resulting from this are shown in Table 3(*a*), column 5. It can be seen that the differences from the result of the 'half'-atom procedure are extremely small (Table 5), the mean differences of coordinates being comparable with the standard deviation of either refinement separately. The mean differences between anorthite and bytownite, shown in the same table, are from three to six times as great. The 'splittings', shown in column 1, are very much larger again.

The resemblance between the results of the two different refinement procedures does not in itself prove the correctness of this particular structure of bytownite, but it does give a strong indication of its physical plausibility. The argument is in two steps. First, the results show that there *is* a unique choice for bytownite, significantly different from anorthite yet with a one-to-one correspondence of all features; the choice is neither a matter of doubtful guesswork nor the result of distinguishing between quantities whose differences are less than experimental error. Secondly, since the 'splittings' have no physical meaning – they represent differences of relative positions of atoms which are really far apart in the structure, in separate half-cells, linked by a non-linear chain of nearest-neighbour bonds – it is extremely unlikely that movements of atomic positions between anorthite and bytownite of magnitude large enough to reverse the sense of the 'splittings' should leave so nearly unaltered the

Table 5. *Differences of coordinates (in fractions of cell edge* $\times 10^4$, *averaged over atoms of same chemical species)*

		Between half-atom sites in bytownite	Between individual atomic sites in anorthite and bytownite	Between two independent refinements of bytownite
Ca/Na	*x*	76	17	5
	y	238	56	10
	z	272	65	10
T	*x*	66	10	3
	y	36	9	2
	z	68	9	3
O	*x*	147	24	7
	y	47	17	3
	z	110	26	6

mean atomic positions. It is much more probable that the movements of all individual atoms are of the same order of magnitude as those of the average positions – the centres of 'half'-atom pairs – and, therefore, that none of the senses of the splittings are reversed. If particular atoms had small splittings and large movements, this argument would not hold for them. In fact the nearest approach to such a condition occurs for some of the O_C atoms, but even for them crossing-over seems improbable, and for most of the atoms quite impossible. Hence there is only one physically reasonable choice for the bytownite structure from among the 2^{25} possibilities allowed by the direct diffraction evidence, namely that whose coordinates are given in Table 3(*b*). In what follows, this will be referred to without qualification as the bytownite structure. It must be remembered that in presenting it as the correct solution we are assuming mistakes of an anti-phase-domain character in order to account for the absence of '*c*' and '*d*' reflexions.

Table 6. *Bond lengths and angles*

(*a*) Ca/Na–O bonds (Å)

Ca/Na(000)			Ca/Na(*zi*0)			Ca/Na(*z*00)			Ca/Na(0*i*0)		
O_A(1000)	2·669		O_A(1*zi*0)	2·387		O_A(1*z*00)	2·434		O_A(10*i*0)	2·439	
O_A(100*c*)	2·526		O_A(1*zic*)	2·727		O_A(1*z*0*c*)	2·853		O_A(10*ic*)	2·845	
O_A(2000)	2·304		O_A(2*zi*0)	2·331		O_A(2*z*00)	2·361		O_A(20*i*0)	2·312	
O_A(2*z*0*c*)		3·527	O_A(20*ic*)		3·956	O_A(2*z*0*c*)		3·310	O_A(20*ic*)		3·308
O_A(200*c*)		3·998	O_A(2*zic*)		3·551						
O_B(000*c*)	2·407		O_B(0*zic*)	2·388		O_B(0*z*0*c*)	2·484		O_B(00*ic*)	2·413	
O_B(*m*00*c*)		3·769	O_B(*mzic*)		2·976	O_B(*mz*0*c*)	2·419		O_B(*m*0*ic*)	2·627	
O_C(0*zi*0)		3·047*	O_C(0000)		3·612	O_C(00*i*0)		3·834	O_C(0*z*00)		3·676
O_C(*mzi*0)		3·302	O_C(*m*000)	2·707		O_C(*m*0*i*0)	2·500		O_C(*mz*00)	2·609	
O_D(0000)	2·447		O_D(0*zi*0)	2·422		O_D(0*z*00)	2·455		O_D(00*i*0)	2·422	
O_D(*m*000)	2·565		O_D(*mzi*0)		3·095*	O_D(*mz*00)		3·844	O_D(*m*0*i*0)		3·697
Mean	2·486 (2·566*)		Mean	2·493 (2·579*)		Mean	2·501		Mean	2·524	

* The corresponding bond-lengths in anorthite were short enough to be included in the left-hand column; if that were done here, the mean values would be those given in brackets.

(*b*) Individual T–O bonds (Å)

Atoms		Length	Atoms		Length
T	O		T	O	
T_1(0000)	O_A(1000)	1·642	T_1(0*z*00)	O_A(1*z*00)	1·773
	O_B(0000)	1·656		O_B(0*z*00)	1·744
	O_C(0000)	1·591		O_C(0*z*00)	1·720
	O_D(0000)	1·593		O_D(0*z*00)	1·729
T_1(00*i*0)	O_A(10*i*0)	1·638	T_1(0*zi*0)	O_A(1*zi*0)	1·749
	O_B(00*i*0)	1·591		O_B(0*zi*0)	1·763
	O_C(00*i*0)	1·607		O_C(0*zi*0)	1·698
	O_D(00*i*0)	1·650		O_D(0*zi*0)	1·786
T_1(*mz*0*c*)	O_A(1*z*00)	1·631	T_1(*m*00*c*)	O_A(1000)	1·760
	O_B(*mz*0*c*)	1·629		O_B(*m*00*c*)	1·669
	O_C(*mz*0*c*)	1·629		O_C(*m*00*c*)	1·728
	O_D(*mz*0*c*)	1·583		O_D(*m*00*c*)	1·753
T_1(*mzic*)	O_A(1*zic*)	1·606	T_1(*m*0*ic*)	O_A(10*ic*)	1·725
	O_B(*mzic*)	1·570		O_B(*m*0*ic*)	1·754
	O_C(*mzic*)	1·627		O_C(*m*0*ic*)	1·747
	O_D(*mzic*)	1·638		O_D(*m*0*ic*)	1·671
T_2(0*z*00)	O_A(2*z*00)	1·631	T_2(0000)	O_A(2000)	1·741
	O_B(0*z*00)	1·625		O_B(0000)	1·682
	O_C(*m*0*i*0)	1·616		O_C(*mzi*0)	1·711
	O_D(*m*00*c*)	1·613		O_D(*mz*0*c*)	1·706
T_2(0*zi*0)	O_A(2*zi*0)	1·630	T_2(00*i*0)	O_A(20*i*0)	1·750
	O_B(0*zi*0)	1·618		O_B(00*i*0)	1·777
	O_C(*m*000)	1·597		O_C(*mz*00)	1·723
	O_D(*m*0*ic*)	1·599		O_D(*mzic*)	1·663
T_2(*m*00*c*)	O_A(200*c*)	1·647	T_2(*mz*0*c*)	O_A(2*z*0*c*)	1·745
	O_B(*m*00*c*)	1·596		O_B(*mz*0*c*)	1·722
	O_C(0*zic*)	1·588		O_C(00*ic*)	1·695
	O_D(0*z*00)	1·599		O_D(0000)	1·755
T_2(*m*0*ic*)	O_A(20*ic*)	1·636	T_2(*mzic*)	O_A(2*zic*)	1·721
	O_B(*m*0*ic*)	1·612		O_B(*mzic*)	1·702
	O_C(0*z*0*c*)	1·593		O_C(000*c*)	1·767
	O_D(0*zi*0)	1·670		O_D(00*i*0)	1·738

Table 6 (*cont.*)

(*c*) O–O distances in tetrahedron edges (Å)

Tetrahedron	O_A–O_B	O_A–O_C	O_A–O_D	O_B–O_C	O_B–O_D	O_C–O_D
$T_1(0000)$	2·577	2·763	2·546	2·658	2·722	2·615
$T_1(00i0)$	2·520	2·740	2·573	2·678	2·671	2·705
$T_1(mz0c)$	2·517	2·755	2·607	2·677	2·708	2·609
$T_1(mzic)$	2·533	2·642	2·570	2·672	2·646	2·671
$T_2(0z00)$	2·621	2·509	2·662	2·663	2·707	2·705
$T_2(0zi0)$	2·627	2·524	2·671	2·690	2·600	2·673
$T_2(m00c)$	2·705	2·549	2·662	2·605	2·579	2·666
$T_2(m0ic)$	2·611	2·594	2·682	2·654	2·722	2·694
$T_1(0z00)$	2·674	2·980	2·699	2·863	2·964	2·837
$T_1(0zi0)$	2·684	2·971	2·614	2·919	2·982	2·902
$T_1(m00c)$	2·774	2·902	2·680	2·793	2·861	2·867
$T_1(m0ic)$	2·671	2·897	2·731	2·893	2·879	2·786
$T_2(0000)$	2·812	2·726	2·756	2·806	2·759	2·854
$T_2(00i0)$	2·726	2·637	2·766	2·918	2·895	2·874
$T_2(mz0c)$	2·817	2·725	2·745	2·812	2·871	2·943
$T_2(mzic)$	2·783	2·748	2·797	2·884	2·822	2·921

(*d*) Bond angles at T (°)

	Edge subtending angle at T					
Atom	O_A–O_B	O_A–O_C	O_A–O_D	O_B–O_C	O_B–O_D	O_C–O_D
$T_1(000)$	102·8	117·5	103·6	109·6	113·3	110·0
$T_1(00i)$	102·5	114·8	102·9	113·3	110·8	111·8
$T_1(mz0)$	100·7	114·8	107·7	110·6	114·7	108·4
$T_1(mzi)$	106·1	110·1	105·2	113·6	111·4	110·1
$T_2(0z0)$	107·3	101·1	109·8	110·8	113·4	113·5
$T_2(0zi)$	107·8	102·6	111·2	113·6	107·9	113·4
$T_2(m00)$	112·8	103·9	110·0	109·6	107·4	113·3
$T_2(m0i)$	106·8	106·9	108·4	111·5	111·7	111·2
$T_1(0z0)$	99·2	117·2	101·1	111·2	117·2	110·5
$T_1(0zi)$	99·4	118·9	95·0	114·9	114·0	112·6
$T_1(m00)$	108·4	112·7	99·4	111·2	113·7	110·9
$T_1(m0i)$	100·3	113·2	107·3	111·6	114·7	109·6
$T_2(000)$	110·6	104·5	106·9	111·4	109·3	113·9
$T_2(00i)$	101·9	99·2	108·3	113·7	114·9	116·2
$T_2(mz0)$	108·2	104·8	103·6	110·4	111·3	117·7
$T_2(mzi)$	108·6	103·8	108·1	112·4	110·5	113·2

(*e*) Bond angles at O (°)

	O_A		O_B	O_C	O_D
1000	139·2	0000	132·5	131·1	133·0
10*i*0	140·8	00*i*0	134·7	129·5	129·0
1*z*00	137·2	0*z*00	139·0	131·5	127·7
1*zi*0	138·5	0*zi*0	131·5	131·8	134·0
2000	126·7	*m*000	168·0	130·9	139·9
20*i*0	123·6	*m*0*i*0	147·9	130·5	159·6
2*z*00	124·7	*mz*00	144·2	128·4	162·2
2*zi*0	125·3	*mzi*0	161·7	132·0	141·9

7. Discussion of the structure

7.1. *Introduction*

Bond lengths and bond angles in Table 6 have been calculated for the final structure, from the coordinates in Table 3(*b*), and the calculated errors also refer to this. Conclusions about Si/Al ordering, which depend on average bond lengths within the tetrahedra, could be drawn either from this structure or from the body-centred approximation, as discussed below. The setting-out of the tables has been arranged to allow easy comparison with the corresponding results for anorthite (Megaw, Kempster & Radoslovich, 1962).

7.2. *Errors*

Errors in coordinates were calculated by Cruickshank's formula [Lipson & Cochran, 1953; formula (308.4)]. The curvature C_n which appears in the formula was calculated from the theoretical *f*-curve for the atom in question, modified by the appropriate temperature factor. It could not be calculated from the F_o maps because peaks on these were averages over two 'half'-sites in all cases. Values of $\sigma(x_n)$ were: for Ca/Na, 0·004 Å; for Si/Al, 0·001 Å; for O, 0·003 Å.

7.3. *Bond lengths and bond angles*

Bond lengths and bond angles are given in Table 6. Estimated errors in bond lengths and angles, calculated from the above values of $\sigma(x_n)$, are as follows: Ca/Na–O, ±0·008 Å; Si/Al–O, ±0·007 Å; O–O, ±0·008 Å; angle at Si/Al, ±0·4°; angle at O, ±0·6°. The standard deviations $\varepsilon(r)$ of the bond lengths within each tetrahedron from the tetrahedral mean are shown in Table 7. Most of these are so much greater than the

error estimated from $\sigma(x_n)$ as to suggest a real variation of bond length within a tetrahedron. Similar real variations were found in anorthite (Megaw, Kempster & Radoslovich, 1962, § 2.1), and have been shown in recent years to be common in many other silicates.

7.4. T–O *bond lengths and* Si/Al *distribution*

At a very early stage of refinement it became clear that T–O tetrahedra were divided into two groups having bond lengths about 1·62 and 1·74 Å. The division became more marked as refinement proceeded. It was plain from consideration of the standard deviations $\varepsilon(r)$ that the difference between the groups was highly significant. Eight tetrahedra, those listed on the left-hand side of Table 7, are Si-rich, with average bond length 1·617 Å; the other eight, on the right-hand side, are Al-rich, with average bond-length 1·732 Å. This division into Si-rich and Al-rich groups was clearly apparent at the body-centred approximation; that it also holds good for all the possible 'half-atom' structures can be seen from Table 4, where none of the different combinations of α and β sites for T and O within a tetrahedron give T–O values sufficiently distinct from each other to change the classification from Si-rich to Al-rich or *vice versa*. In any of the 2^{25} 'structures' allowed by the diffraction evidence, therefore, the Si/Al ordering in bytownite is to a first approximation complete, and the pattern is identical with that in anorthite, the Si-rich and Al-rich tetrahedra alternating throughout the structure.

Whether, at the second approximation, there is any residual Si/Al disorder, or any regularity in the distribution of Si in Al-rich sites, is a more difficult question, and for this the final structure whose bond-lengths are given in Table 6 must be considered. It is commonly accepted (see *e.g.*, Brown & Bailey, 1964; Appleman & Clark, 1965) that the mean value of T–O for a tetrahedron gives a good measure of the atomic content on a linear scale from Si to Al, even though the four individual values have a very considerable scatter; Smith & Bailey (1963) in giving 1·61 and 1·75 Å as the extreme values suggest that local effects may produce errors of ±5% in the estimated Al content, but Appleman & Clark prefer to allow ±8%, *i.e.* to disregard differences less than 0·012 Å in tetrahedral means. In bytownite (as in anorthite) there are sufficient different tetrahedra to allow an empirical study of the relation of irregularity and scatter.

We describe irregularity of a tetrahedron in terms of T–O distances rather than O–O distances, because the latter combine the effect of T–O bonds and O–T–O bond angles, which are more conveniently kept as separate variables. The irregularity is measured by the differences $\delta(r)$ of individual bonds from the tetrahedral mean r_t, or by the r.m.s. value of the $\delta(r)$'s for the tetrahedron, $\varepsilon_t(r)$. This is to be compared with the scatter of the tetrahedral means about the group mean, examining either their individual deviations $\delta(r_t)$ or the r.m.s. value $s(r_t)$. These are all listed in Table 7.

If all the values of $\delta(r)$ in the group were random and independent, the scatter index $s(r_t)$ could be predicted from the $\delta(r)$'s; denoting by $\varepsilon_g(r)$ the r.m.s. value of $\delta(r)$ for the group, the ratio $s(r_t)/\frac{1}{2}\varepsilon_g(r)$ would be unity if all the tetrahedra were statistically alike, and greater than unity if they were really different. From Table 7 it can be seen that in all cases the ratio is considerably *less* than unity – most strikingly so for the Al-rich tetrahedra in anorthite. Hence the postulate of random deviations $\delta(r)$ within a tetrahedron must be incorrect; there must be some physical effect tending to make the mean value of the T–O bonds 'correct' for the particular kind of T atom, even at the expense of considerable inequalities in the separate bond lengths. The effect is most clearly displayed in anorthite, where the residual disorder (if any) is too small to make any other explanation plausible; but it can

Table 7. *Comparison of bytownite and anorthite* T–O *bond lengths: tetrahedral means* r_t, *standard deviations within a tetrahedron* $\varepsilon(r)$, *and deviations of tetrahedral means from group means,* $\delta(r_t)$

Atom	Si-rich group						Atom	Al-rich group					
	Bytownite			Anorthite				Bytownite			Anorthite		
	Length r_t (Å)	$\varepsilon(r)$	$\delta(r_t)$	Length r_t (Å)	$\varepsilon(r)$	$\delta(r_t)$		Length r_t (Å)	$\varepsilon(r)$	$\delta(r_t)$	Length r_t (Å)	$\varepsilon(r)$	$\delta(r_t)$
$T_1(0000)$	1·620	0·029	+0·003	1·613	0·031	−0·001	$T_1(0z00)$	1·742	0·020	+0·012	1·758	0·034	+0·009
$T_1(00i0)$	1·622	0·024	+0·005	1·616	0·029	+0·002	$T_1(0zi0)$	1·749	0·032	+0·019	1·746	0·032	−0·003
$T_1(mz00)$	1·618	0·020	+0·001	1·608	0·022	−0·006	$T_1(m000)$	1·738	0·033	−0·001	1·752	0·027	+0·003
$T_1(mzi0)$	1·610	0·026	−0·007	1·626	0·017	+0·012	$T_1(m0i0)$	1·724	0·033	−0·006	1·741	0·027	−0·008
$T_2(0z00)$	1·621	0·007	+0·004	1·613	0·015	−0·001	$T_2(0000)$	1·710	0·021	−0·020	1·746	0·024	−0·003
$T_2(0zi0)$	1·611	0·014	−0·006	1·610	0·031	−0·004	$T_2(00i0)$	1·728	0·042	−0·002	1·753	0·039	+0·004
$T_2(m000)$	1·608	0·023	−0·009	1·602	0·031	−0·012	$T_2(mz00)$	1·728	0·023	−0·002	1·744	0·023	−0·005
$T_2(m0i0)$	1·628	0·029	+0·011	1·628	0·004	+0·014	$T_2(mzi0)$	1·732	0·024	+0·002	1·752	0·038	+0·003
Mean	1·617			1·614			Mean	1·732			1·749		
$\varepsilon_g(r)$		0·023			0·024				0·030			0·031	
$S(r_t)$			0·0069			$0·008_2$				$0·011_0$			$0·005_3$
$S(r_t)/\frac{1}{2}\varepsilon_g(r)$			0·60			0·68				0·73			0·34

$\varepsilon_g(r)$ is the *r.m.s.* value over the whole group of $\varepsilon(r)$, or of the individual $\delta(r)$'s.
$S(r_t)$ is the *r.m.s.* value of the $\delta(r_t)$'s for the group.

also be recognized when some Si/Al replacement occurs. The effect does not mean that, for example, in bytownite, all Al-rich tetrahedra will be equally receptive to the excess Si; it *does* mean that they will show their true Si-content more accurately by their tetrahedral means than might have been predicted from their irregularity. Indeed, the greatly increased scatter of Al-rich tetrahedra in bytownite as compared with anorthite, without increased irregularity, is clear evidence that they differ in their Si-content. That the scatter is greater for Si-rich tetrahedra in both materials than for the Al-rich tetrahedra in anorthite may have one of two explanations. Either there is a genuine difference between tetrahedra, because of residual Si/Al disorder in both materials affecting certain sites preferentially; or the greater strength of Si–O bonds compared with Al–O means that their individual lengths are less adaptable and stresses less easily averaged out within the tetrahedron. Possibly both causes are at work.

Tentatively we assume that 'strain effects' may produce variations in tetrahedral means of about $\pm 0{\cdot}007$ Å, corresponding to the $\pm 5\%$ variation in apparent site-content suggested by Smith & Bailey (1963), and we regard differences from this limit up to $\pm 0{\cdot}014$ Å as only doubtfully significant (not distinguishing between Si-rich and Al-rich sites, though actually the latter are likely to be more sensitive).

This allows a rough quantitative estimate of site contents to be made from Table 7. In bytownite, three Al-rich sites differ notably from the rest: $Al_1(0zi0)$, which contains no Si, $Al_1(0z00)$ which has below-average Si, and $Al_2(0000)$ which has above-average Si; the occupancies are approximately 0, 6 and 30% respectively in these three, and 13% in all the others. The distinctiveness of the second-named is borderline; for the other two it is quite marked, their $\delta(r)$'s being three times as great as the r.m.s. value for the other six. The bytownite Si-rich sites, by contrast, show only one, $Si_2(m0i0)$, with any Al content, and that is doubtfully significant at 10%. In anorthite a similar treatment indicates that both $Si_2(m0i0)$ and $Si_1(mzi0)$ have a 10% Al content; apparently the excess Si in bytownite replaces all the Al in the latter site leaving the former unaffected. No explanation is offered at this stage; all the differences in Si-rich tetrahedra are so close to the order of magnitude of the strain effects that one cannot be sure of the reality of occupancy differences. The overall group figures for means of Si-rich and Al-rich sites in bytownite offer no clearer evidence: the small increase for Si-rich tetrahedra from anorthite to bytownite would correspond to a 2·5% decrease in Si-content, and the decrease for Al-rich tetrahedra to a 13% increase in Si-content, as compared with the net figure of 10% expected from the composition. Though these figures, averaged over eight tetrahedra in each group, have a lower average strain error than individual tetrahedral means, it is still too high for the evidence of residual Al/Si disorder to be more than doubtfully significant, particularly as it is not clear what allowance should be made for the additional strains due to anti-phase-domain boundary effects.

A further point to bear in mind in any comparison of Si/Al ordering in anorthite and bytownite is the possible discontinuity in structure at $An_{90\text{-}95}$ suggested by the graph of γ^* against composition for low plagioclases plotted by Doman, Cinnamon & Bailey (1965). If this is substantiated when more examples are available, it could mean that changes in the relative occupancies of T-sites between anorthite and bytownite might follow one sequence from An_{100} to $An_{90\ 95}$ and another thereafter.

7.5. A–O *bond-lengths and the environment of the* A *atoms*

Table 6(*a*) lists A–O bond lengths for the particular solution of bytownite. Bond lengths less than 2·9 Å are listed on the left hand side of the columns, other distances less than 4 Å are assumed to be non-bonding contacts, and are listed on the right. The choice of a limit distinguishing 'neighbours' from non-bonding contacts is always somewhat arbitrary when the environment of the cation is irregular, as it is here; the corresponding choice in anorthite was at 3·1 Å, but here 2·9 Å seemed to mark a more natural break. The atoms Ca/Na(000) and (*zi*0) are then classed as 6-coordinated, while Ca/Na(*z*00) and (0*i*0) are 7-coordinated. The chief qualitative differences from anorthite are the much increased irregularity between the two $O_A(1)$ bonds for Ca/Na(*zi*0), and also (to a slightly less degree) for Ca/Na(*z*00); and the reduction of the inequality between the $O_B(mzic)$ and $O_D(mzi0)$ bonds for Ca/Na(*zi*0), which leaves them both just outside the bonding limit of 2·9 Å. All bonds from Ca/Na to $O_A(2)$ are noticeably shorter than to the other O's (less than 2·37 Å in every case). This is a common feature of most feldspars; cation bonds to $O_A(2)$ always seem to be short (*cf.* in particular Megaw, Kempster & Radoslovich, 1962, § 2.2).

As well as resembling one another in being approximately 6-coordinated, Ca/Na(000) and Ca/Na(*zi*0) are also similar in other respects. Reference to Fig. 6, which shows the composite Ca/Na(000) and (0*i*0) peak on the body-centred electron-density map of bytownite, indicates that Ca/Na(000) is a lower peak (peak height $26{\cdot}6 \pm 2$ e.Å^{-3}) than Ca/Na(0*i*0) (peak height $34{\cdot}7 \pm 2$ e.Å^{-3}). The composite Ca/Na(*z*00) and (*zi*0) peak on the other hand is unresolved, and peak heights for the two constituent peaks cannot be obtained directly. When, however, profiles of the two peaks Ca/Na (000) and (0*i*0) were obtained by interpolation and moved together from their 0·85 Å separation in the composite peak to one of 0·43 Å [the separation of the two 'half'-peaks Ca/Na(*z*00) and (*zi*0)], a very good fit was obtained to the pear-shaped profile. This goodness of fit suggests that Ca/Na(000) and (*zi*0) have similar profiles, as have Ca/Na(*z*00) and (0*i*0). The

composite Ca/Na(z00) and (zi0) peak is pear-shaped because the two constituent half-atom peaks are too close together (0·43 Å) to be well resolved. Ca/Na atoms therefore fall into two groups: Ca/Na(000), (zi0) with peak heights 27 e.Å^{-3} and 6-coordination of oxygen; Ca/Na(z00), (0i0) with peak heights 35 e.Å^{-3} and 7-coordination of oxygen. The lower peak height of the former pair may mean that there is a tendency for Na to concentrate in it; quantitatively the difference is just greater (but not significantly so) than what would be predicted if all the Na atoms were in the pair 000/zi0. If so, the 6-coordination (or the geometrical environment and mean A–O distance summed up by that term) may be a cause and not a consequence of the Na occupancy, because a similar geometrical difference between the pairs has been noted in anorthite (Megaw, Kempster & Radoslovich, 1962, p.1024).

Alternatively the difference in peak heights might be a consequence of different thermal amplitudes, themselves a consequence of the geometrically different environments of the pairs of atoms. The temperature factors of the different A atoms were not refined separately, but had a mean isotropic value of $B=0{\cdot}90$ Å^2. In anorthite (Kempster, 1957) the separate pairs (000)/(zi0) and (0i0)/(z00) had values of 1·0 and 0·3 Å^2; in transitional anorthite (Ribbe & Megaw, 1962) provisional values were given as 1·8 and 0·3 Å^2 respectively. It seems likely that the underlying cause of the difference between pairs is the same in all three materials. That it is a consequence of thermal amplitudes depending on interatomic forces in the perfect structure cannot be ruled out. But there is an interesting alternative possibility. In bytownite and transitional anorthite there are anti-phase-domain boundaries. These, we suggest, though irregular in their contours, are located at specific places in the unit cell, cutting across the weakest bonds of the perfect structure. At present we do not know where these breaks occur. But if they lay near the A (000)/(zi0) atoms and remote from the A (0i0)/(z00) the former pair would show greater position disorder. The boundary – or considerable areas of it – would then lie parallel to (001) at $z=0$. This suggestion – which is only a speculation – is not necessarily an alternative to the suggestion of different thermal amplitudes in the perfect structure, but might enhance their effect, because large thermal amplitudes indicate weak forces and therefore mark the most favourable location for a fault. Indeed, in bytownite all three explanations could be true, because the region of a fault might be the preferred site for the Na atom.

The average isotropic value of the temperature factor for oxygen atoms is 1·06 Å^2. This was estimated at the final stage of refinement with the body-centred oxygen coordinates. It will therefore contain a disorder contribution because each oxygen site is an average over two half-sites. No revised estimates were made later during refinement with half-atoms. It is not then possible to say how much of the value 1·06 Å^2 corresponds to thermal motion.

7.6. O–O *distances, and bond angles at* Si, Al *and* O

O–O distances and bond angles are recorded in Table 6(c), (d) and (e). The standard error in bond angles is about 0·6° and differences of angles from the tetrahedral values are therefore real. Bond angles at O are similar to those in anorthite (*cf.* Megaw, Kempster & Radoslovich, 1962; Table 2).

8. Comparison of 'irregularities' and 'strains' in various feldspars

8.1. T–O *bond lengths*

It is of interest to try and explain the differences of individual bond lengths from those expected from the occupancy of the site. There are two possible causes: (i) local attractive forces between an oxygen atom and its Ca/Na neighbours, tending to lengthen the T–O bonds, (ii) 'structural stresses' due to the tie-up as a whole, and not easy to analyse into their component factors – though one such factor, common to all feldspar structures, was detected by its effect on bond-angle strains in anorthite (Megaw, Kempster & Radoslovich, 1962) and given a physical explanation in terms of Ca–Ca repulsion. We shall consider (i) and (ii) separately.

There is a positive correlation in bytownite, as in anorthite, between the length of a T–O bond and the number of its Ca/Na neighbours. This is displayed in Table 8. The values are very like those for anorthite; the differences between the groups are marginally smaller.

Table 8

(a) Classification of oxygen atoms according to number of Ca/Na neighbours

	Number of neighbours	Atoms	Number of atoms in group
Group 1	2	$O_A(100)$ $O_A(10i)$ $O_A(1z0)$ $O_A(1zi)$	4
Group 2	1	$O_A(200)$ $O_A(20i)$ $O_A(2z0)$ $O_A(2zi)$ $O_B(000)$ $O_B(00i)$ $O_B(0z0)$ $O_B(0zi)$ $O_B(m0i)$ $O_B(mz0)$ $O_C(m00)$ $O_C(m0i)$ $O_C(mz0)$ $O_D(000)$ $O_D(00i)$ $O_D(0z0)$ $O_D(0zi)$ $O_D(m00)$	18
Group 3	0	$O_B(m00)$ $O_B(mzi)$ $O_C(000)$ $O_C(00i)$ $O_C(0z0)$ $O_C(0zi)$ $O_C(mzi)$ $O_D(m0i)$ $O_D(mz0)$ $O_D(mzi)$	10

(b) Mean bond lengths for the groups

	Mean bond length (Å)		S.D. of mean bond length (Å)	
	Si–O	Al–O	Si–O	Al–O
Group 1	1·629	1·752	0·007	0·009
Group 2	1·625	1·742	0·005	0·006
Group 3	1·599	1·700	0·006	0·009

This kind of correlation has *not* been observed in the 7 Å feldspars; for maximum microcline (Brown & Bailey, 1964) there appears to be a correlation, but in the opposite sense – lengthened T–O bonds for *smaller* numbers of K neighbours – and for low albite and reedmergnerite (Appleman & Clark, 1965) there is no

obvious correlation. (High albite cannot be used as evidence, because of the uncertainty about the Na environment.) It is, therefore, interesting to try another approach.

For this, the average $\delta(r)$ of the two T–O bonds to an oxygen is plotted against the distance of the nearest Ca/Na neighbour (Fig. 8). Each $\delta(r)$ is the deviation of the bond from the mean of its *own* tetrahedron. The average of the two, δ(O), which [like $\delta(r)$] may be of either sign, is a measure of the mean outward strain at the oxygen referred to an arbitrary 'unstrained' length, and therefore is expected to increase as the distance to a single nearest neighbour decreases, or the number of equally near neighbours increases. Fig. 8 shows all the points for anorthite and bytownite. Their general trend is obvious. There is no theory from which to predict the shape of the curve, but it is fitted by the function $y=2{\cdot}28+(0{\cdot}04-x)^3\times 3{\cdot}7$ (chosen because a cubic seemed the simplest function of approximately the right shape). This is shown by the full line; the dotted lines are separated from it by twice the standard deviation of δ(O), as estimated from $\sigma(\varrho)$. Errors of measurement of y are negligible.

Not all the departures from the curve can be explained, but the effects for the $O_A(1)$ atoms are of particular interest. Those that have two nearest neighbours at nearly equal distances less than 2·70 Å [$O_A(100)$ in bytownite, and $O_A(100)$ and $O_A(1z0)$ in anorthite] lie above the curve in a group near $\delta(O)=\pm 0{\cdot}035$, r(Ca–O) = 2·5. The rest, with one near neighbour at about 2·5 Å and a more distant one at 2·7–2·8 Å, lie within or close to the area of the main sequence.

It is rather difficult to assess the significance of this correlation, because it might be an indirect one, due to the dependence of both δ(O) and the Ca/Na–O distances on some 'structural stress' system rather than to a direct nearest-neighbour attraction. A similar analysis carried out for the 7 Å feldspars gives no agreement. There are two reasons for thinking that direct attraction might be relatively more important in the 14 Å feldspars than in the 7 Å group: the direct forces involved are larger because of the high valency of the A cation (and, relative to microcline, because of the very much shorter A–O distance), and the structural stresses are probably smaller (at least relatively), because the greater number of symmetry-independent tetrahedra in the repeat unit allows them more chance to even themselves out. Moreover, as we shall show below, some of the structural stress factors appear to be quite different in the two groups.

Structural strains in individual T–O bonds can most easily be examined in terms of $\delta(r)$, the departure of each bond from its own tetrahedral mean. This eliminates the effective bond-length differences due to different occupancies, and enables us to discuss the irregularities of tetrahedra in terms of their topological role in the framework. Inspection shows that differences in $\delta(r)$'s between tetrahedra containing chemically different atoms are not so great that they have to be taken into account at this stage.

Correlation coefficients between $\delta(r)$'s for corresponding bonds in the 7 Å structure showed a very striking resemblance between low albite, reedmergnerite and maximum microcline (Table 9). The calculation

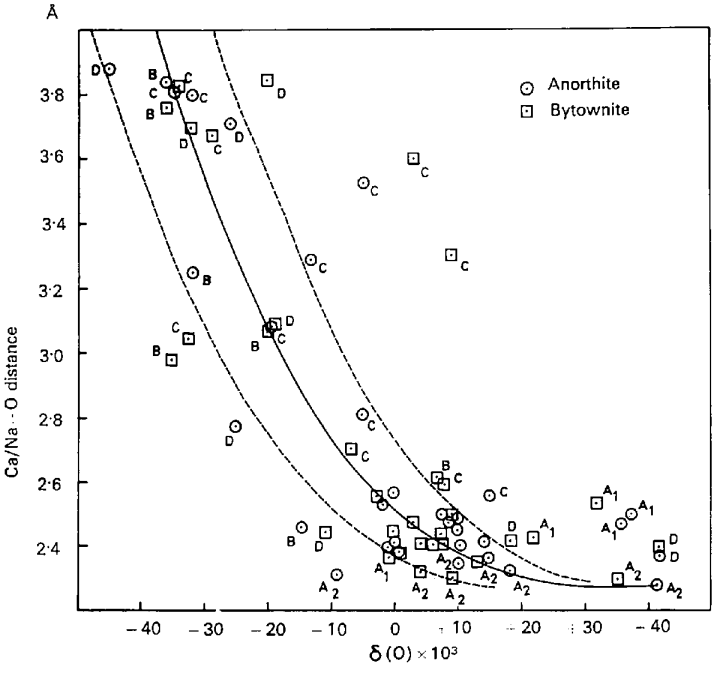

Fig. 8. Variation of Ca/Na–O distance with average deviation δ(O) of T–O bonds to same O atom from their tetrahedral means. Full line is empirically fitted cubic; dotted lines indicate standard deviation from it. Points not in the most crowded region are marked with the symbol of the O atom concerned.

was carried out over all four tetrahedra, irrespective of their contents – a comparison of 16 bonds from each structure. It is surprising to find the detail of the irregularities so little affected by the replacement of a large Al atom by a small B, or a medium-sized Na by a large K. Obviously the irregularities must here be mainly due to a structural stress system, inherent in the linkage pattern. Does the same stress system operate in the 14 Å feldspars? The basis of comparison is not so easy, because there is no obvious degree of uniformity within the sets of four tetrahedra in the 14 Å structures which become identical in the 7 Å structures. Nevertheless, an average $\delta(r)$ was taken for each bond over the four $T_1(0)$ tetrahedra and similarly over $T_1(m)$, $T_2(0)$ and $T_2(m)$, both for anorthite and bytownite, and the averages were compared with $\delta(r)$ for low albite. The correlation factors are given in Table 9. Their evidence is unmistakable. The irregularities of anorthite are quite different from those of low albite. That this distinction is not an artefact from the process of averaging over four tetrahedra is shown by the expected high correlation between anorthite and bytownite, which were both averaged in this way, and also by the good correlation with high albite. The resemblance of high albite to anorthite, and its difference from low albite, have been pointed out by various workers*; what we have done here is to show that the resemblance involves a similar distribution of structural strains, and therefore presumably of structural stresses, and that it can be expressed quantitatively in terms of the individual bond-length strains.

Table 9. *Correlation coefficients for* $\delta(r)$

(For the 14 Å primitive feldspars, the value used for $\delta(r)$ in the correlation is a mean over the four tetrahedra which become identical in the 7 Å base-centred feldspars)

	Correlation coefficients	
	Anorthite	Low albite
Anorthite	—	0·24
Bytownite	0·88	—
High albite	0·63	0·25
Low albite	0·24	—
Maximum microcline	—	0·74
Reedmergnerite	—	0·80

8.2. *Bond angles at* O

Values of bond angles at O atoms follow the expected pattern for 14 Å feldspars, a pattern that has been outlined by Megaw, Kempster & Radoslovich [1962, § 3.3(i.)] At $O_A(1)$ the angles are similar to each other and each slightly greater than the corresponding angle in anorthite. At $O_A(2)$ they are again similar to each other, and all but one are slightly greater than for anorthite, though the differences are smaller than at $O_A(1)$. At O_C they are similar to each other, and the differences from anorthite are small and irregular. At O_B and O_D there is the usual large spread in angles, the largest angles again occurring at those O with no Ca/Na neighbours. The average values at both O_B and O_D are, however, very nearly the same as for anorthite, though individual differences are quite large (nearly twice as great, on the average, for O_D as for O_B); as another example of smoothing-out effects, perhaps attributable to disorder, we note that in bytownite the means for $O_B(0)$ and $O_B(m)$ are each nearer to their common mean than in anorthite, and similarly for $O_C(0)$ and $O_C(m)$, $O_D(0)$ and $O_D(m)$.

8.3. *Bond-angle strains at* T; *and* O–O *tetrahedral edge strains*

Values of angle and edge strains, taken as departures from the values for completely regular tetrahedra, are given in Table 10. The values may be directly compared with those of other feldspars given in Table 10 of Megaw, Kempster & Radoslovich (1962.) Bond-angle strains at all T atoms of the same crystallographic type, T_1 or T_2, show marked similarity. This is clearly a common feature of all feldspars, independent of symmetry or Si/Al ratio. The four largest strains are in the same place as in all other feldspars: in $T_1(AB)$, $T_1(AC)$, $T_1(AD)$ and $T_2(AC)$. The Al-rich tetrahedra as before show greater strains than the Si-rich. Comparing bytownite with anorthite, one finds the following differences:

(i) The overall average magnitudes of the strains are slightly less in bytownite.

(ii) The scatter within the groups averaged in Table 10 is quite appreciably less for bytownite, but obviously correlated with that for anorthite, groups which were non-uniform in anorthite becoming only a little more uniform in bytownite.

(iii) The differences of individual bond angles from anorthite to bytownite are very much less than the strains, of order of magnitude equal to about half the r.m.s. scatter of the strains about the group means.

Table 10. *Bond angle strains* (°) *and* O–O *tetrahedron edge strains* (Å)

Strains are deviations from values for a regular tetrahedron. The table lists the means over corresponding angles and edges in similar tetrahedra, and their standard deviations.

Type of tetrahedron		O–T–O angle Si	O–T–O angle Al	O–O edge Si	O–O edge Al
T_1	*AB*	−6·5	−7·7	−0·103	−0·124
		±0·9	±1·9	±0·012	±0·021
	AC	+4·8	+6·0	+0·83	+0·115
		±1·3	±1·3	±0·023	±0·020
	AD	−4·7	−8·8	−0·66	−0·144
		±0·9	±1·3	±0·011	±0·021
	BC	+2·3	+2·7	+0·031	+0·042
		±0·9	±0·8	±0·004	±0·023
	BD	+3·1	+5·4	+0·047	+0·097
		±0·8	±0·7	±0·015	±0·026
	CD	+0·6	+1·4	+0·010	+0·023
		±0·6	±0·6	±0·020	±0·021
T_2	*AB*	−0·8	−2·2	+0·001	−0·026
		±1·2	±1·4	±0·018	±0·018

* Comparisons using structure amplitudes and atomic parameters have been made by Ribbe (1963), with results very similar to ours using bond length strains. See also Srinivasan & Ribbe (1965).

Table 10 (*cont.*)

	Si	Al	Si	Al
AC	−5·9	−6·4	−0·096	−0·099
	±1·1	±1·2	±0·016	±0·021
AD	+0·4	−2·8	+0·039	−0·042
	±0·5	±0·9	±0·006	±0·009
BC	+1·9	+2·5	+0·015	+0·047
	±0·7	±0·6	±0·015	±0·023
BD	+0·5	+2·0	+0·012	+0·029
	±1·3	±1·0	±0·031	±0·026
CD	+3·4	+5·8	+0·044	+0·090
	±0·5	±0·9	±0·008	±0·018

As in other feldspars, there appears to be a strong Ca/Na–Ca/Na repulsion across the symmetry centre. Prediction of bond-angle strains in O–Si–O and O–Al–O angles, made by Megaw, Kempster & Radoslovich (1962) for any feldspar by considering the effect of cation repulsion on the x^* repeat distance, are compared with observed bytownite strains below:

	Mean bond-angle strains (°)					
	$T_1(BC)$	$T_1(BD)$	$T_2(AC)$	$T_2(BC)$	$T_2(BD)$	$T_2(CD)$
Pred.	+	+	−	+	indet.	+
Obs.	+2·6	+4·6	−6·2	+2·2	+1·3	+4·6

The agreement is very satisfactory, but not surprising in view of the close resemblance of anorthite to bytownite. It is perhaps worth noting that the uniformity of the group is greater for these six bond-angle strains than for the rest: the r.m.s. value of the standard deviations of the six is 0·65° for both anorthite and bytownite, against 1·1 and 0·8° respectively for the remaining bond angles. When, as in this case, the stresses which are the main cause of the strains have been identified and found to be in the same sense in corresponding parts of the structure, it is to be expected that the strains will be more uniform than are those associated with stresses which help to differentiate between the subcells.

8.4. *General comment*

In some ways, the very close resemblance of bytownite to anorthite is a disappointment, because when all differences are so small it is hard to pick out those which are physically significant. From one point of view, the bytownite determination serves rather as an independent confirmation of the reality of the detailed features of the anorthite structure than as an exhibition of qualitatively or even quantitatively new effects. There is no doubt, however, that the differences are significant mathematically, and future work may perhaps bring to light some pattern in them which will help to elucidate the nature of the forces operative in both structures.

We wish to thank Dr W. H. Taylor and other colleagues in the Department for interest and encouragement. In particular we are indebted to Dr M. Wells, who wrote the three-dimensional refinement program with which many feldspar refinements have now been completed. Dr M. V. Wilkes kindly gave us permission to use Edsac II. One of us (S.G.F.) acknowledges receipt of a D.S.I.R. Studentship, and another (S.C.) an 1851 Exhibition, during the tenure of which this work was carried out.

References

APPLEMAN, D. E. & CLARK, J. R. (1965). *Amer. Min.* **50**, 1827.

BROWN, B. E. & BAILEY, S. W. (1964). *Acta Cryst.* **17**, 1391.

COCHRAN, W. (1951). *Acta Cryst.* **4**, 81.

COLE, W. F., SÖRUM, H. & TAYLOR, W. H. (1951). *Acta Cryst.* **4**, 20.

CROWFOOT, D., BUNN, C. W., ROGERS-LOW, B. W. & TURNER-JONES, A. (1949). *The X-ray Crystallographic Investigation of the Structure of Penicillin.* Oxford Univ. Press.

DOMAN, R. C., CINNAMON, C. G. & BAILEY, S. W. (1965). *Amer. Min.* **50**, 724.

FERGUSON, R. B., TRAILL, R. J. & TAYLOR, W. H. (1958). *Acta Cryst.* **11**, 331.

FLEET, S. G. (1961). Ph. D. Dissertation, Cambridge University.

FORSYTH, J. B. & WELLS, M. (1959). *Acta Cryst.* **12**, 412.

HOWELLS, E. R., PHILLIPS, D. C. & ROGERS, D. (1950). *Acta Cryst.* **3**, 210.

KEMPSTER, C. J. E. (1957). Ph.D. Dissertation, Cambridge University.

KEMPSTER, C. J. E., MEGAW, H. D. & RADOSLOVICH, E. (1962). *Acta Cryst.* **15**, 1005.

LIPSON, H. & COCHRAN, W. (1953). *The Determination of Crystal Structures.* London: Bell.

MACKENZIE, W. S. (1960). Abstract of discussion on nomenclature, held at the symposium on feldspars, Copenhagen.

MEGAW, H. D. (1956). *Acta Cryst.* **9**, 56.

MEGAW, H. D. (1960). *Proc. Roy. Soc.* A,**259**, 184.

MEGAW, H. D., KEMPSTER, C. J. E. & RADOSLOVICH, E. (1962). *Acta Cryst.* **15**, 1017.

PHILLIPS, D. C. (1956). *Acta Cryst.* **9**, 819.

RAMACHANDRAN, G. N. & SRINIVASAN, R. (1959). *Acta Cryst.* **12**, 410.

RIBBE, P. H. (1963). Thesis, p.242, Cambridge University.

RIBBE, P. H. & MEGAW, H. D. (1962). *Norsk. Geologisk Tidsskrift*, **42**, (2), 158.

SMITH, J. V. & BAILEY, S. W. (1963). *Acta Cryst.* **16**, 801.

SÖRUM, H. (1951). K. norske. vidensk. Selsk. Skr. No. 3. (Doctorate thesis, Trondheim).

SRINIVASAN, R. & RIBBE, P. H. (1965). *Z. Kristallogr.* **121**, 34.

WEISZ, O., COCHRAN, W. & COLE, W. F. (1948). *Acta Cryst.* **1**, 83.

WELLS, M. (1961). Ph.D. Dissertation, Cambridge University.

WILLIAMS, P. P. & MEGAW, H. D. (1964). *Acta Cryst.* **17**, 882.